PNAS RESEARCH ARTICLE | MICROBIOLOGY OPEN ACCESS

RNA-targeted proteomics identifies YBX1 as critical for efficient HCMV mRNA translation

Rebekah J. Dickmander[a], Erik M. Lenarcic[a], John D. Sears[a], Andrew E. Hale[a], and Nathaniel J. Moorman[a,1]

Edited by Thomas Shenk, Princeton University, Princeton, NJ; received October 15, 2024; accepted January 17, 2025

Viruses have evolved unique strategies to circumvent host control of protein synthesis and enable viral protein synthesis in the face of the host response. Defining the factors that regulate viral messenger RNA (mRNA) translation is thus critical to understand how viruses replicate and cause disease. To identify factors that might regulate viral mRNA translation, we developed a technique for identifying proteins associated with a native RNA expressed from its endogenous promoter and genomic locus. This approach uses a guide RNA to target dCas13b fused to a biotin ligase domain to a specific RNA, where it covalently labels proteins in close proximity. Using this approach, we identified multiple proteins associated with transcripts encoding the human cytomegalovirus (HCMV) IE1 and IE2 proteins and found that several associated proteins positively or negatively regulate HCMV replication. We confirmed that one such protein, the cellular Y-box binding protein 1 (YBX1), binds to HCMV immediate early mRNAs and is required for efficient viral protein expression and virus replication. Ablating YBX1 expression reduced the association of HCMV immediate early mRNAs with polysomes, demonstrating a role for YBX1 as a positive regulator of viral RNA translation. These results provide a powerful tool for unraveling RNA–protein interactions that can be used in a wide range of biological processes and reveal a role for YBX1 as a critical regulator of HCMV immediate early gene expression.

RNP proteomics | RNA-binding proteins | mRNA translation | human herpesvirus | protein synthesis

Significance

Human cytomegalovirus (HCMV) infects the majority of people worldwide and can cause severe disease in newborns and immune-compromised individuals. There is no vaccine to prevent HCMV infection, and current treatments have significant limitations, creating an urgent need to discover new targets for novel HCMV therapeutics. Here, we developed a method to identify proteins that interact with viral RNAs in their native context and identified the cellular Y-box binding protein 1 (YBX1) RNA-binding protein as a key positive regulator of translation of mRNAs encoding HCMV immediate early RNAs and virus replication. These data provide a tool for identifying RNA:protein interactions in a physiologically relevant context and the rationale for developing YBX1 inhibitors as therapeutics for HCMV disease.

Human cytomegalovirus (HCMV) is an opportunistic betaherpesvirus that infects the majority of the human population by adulthood, with at least 60% prevalence in developed countries and over 90% in developing countries (1). HCMV infection is typically asymptomatic in healthy individuals but can cause severe disease in neonates (2–4) and in immunocompromised patients (5–8). To date, no approved vaccine exists to prevent HCMV infection or disease (9–15). Current therapeutics are not recommended for use during pregnancy due to limited safety and efficacy data (16, 17) or embryonic toxicity in preclinical studies (18, 19). Likewise, toxicity, adverse events, and antiviral resistance (20–22) limit the use of current therapeutics in immunocompromised patients. Safe and effective therapeutics are therefore urgently needed to treat HCMV disease in at-risk populations.

During lytic infection, HCMV gene expression occurs in a temporal cascade of three kinetic classes of viral genes: immediate-early (IE) genes, early (E) genes, and late (L) genes (23–25). HCMV immediate early genes are rapidly transcribed upon uncoating of the viral genome in the nucleus, and typically act to modulate the cellular response to infection and facilitating the expression of viral early genes. Two critical HCMV genes, UL123 and UL122, encode the IE1 and IE2 proteins respectively, which each play critical roles in the earliest stages of infection. IE2 is essential for HCMV replication, as deletion or disruption of the UL122 gene results in a failure to express viral early genes (26, 27). Disruption or deletion of UL123 is tolerated at a high multiplicity of infection (MOI), but results in a significant growth defect at lower MOIs (28). Both IE1 and IE2 are expressed to high levels within hours of infection and together act to induce the expression of viral and cellular genes required for virus replication (25). IE1 is involved in histone deacetylation (29) and modulation of the type I interferon response (30–33), and with IE2 promotes HCMV replication by stimulating the transcription of viral (34–40) and host (41–45) genes. Understanding the regulation of IE1 and IE2 expression is thus an important step in understanding the mechanisms underlying HCMV replication and pathogenesis.

While the transcriptional regulation of IE1 and IE2 expression has been well studied (46–66), posttranscriptional events also regulate IE1 and IE2 protein levels during infection. Transcripts encoding IE1 or IE2 are differentially associated with polysomes during different stages of infection, suggesting temporal regulation of translation also controls

Author affiliations: [a]Department of Microbiology and Immunology, Lineberger Comprehensive Cancer Center, University of North Carolina at Chapel Hill, Chapel Hill, NC 27599

Author contributions: R.J.D., E.M.L., J.D.S., A.E.H., and N.J.M. designed research; R.J.D., E.M.L., J.D.S., and A.E.H. performed research; R.J.D. contributed new reagents/analytic tools; R.J.D. and N.J.M. analyzed data; and R.J.D. and N.J.M. wrote the paper.

The authors declare no competing interest.

This article is a PNAS Direct Submission.

[1]To whom correspondence may be addressed. Email: nmoorman@med.unc.edu.

This article contains supporting information online at https://www.pnas.org/lookup/suppl/doi:10.1073/pnas.2421155122/-/DCSupplemental.

Published March 4, 2025.

IE1 and IE2 expression (59). The shared major immediate early 5' untranslated region (MIE 5' UTR) of transcripts derived from the MIEP also regulates IE1 and IE2 expression by promoting the efficient translation of the UL122 and UL123 mRNAs during infection (67). Presumably, this effect is due to interaction with specific factors that enhance ribosome recruitment, however, the mechanism by which the MIE 5' UTR enhances UL122 and UL123 mRNA translation has not been defined.

To begin to understand how the MIE 5' UTR regulates the translation of UL122 and UL123 transcripts, and thus IE1 and IE2 protein expression, we developed a proteomics approach to specifically identify proteins that bind the MIE 5' UTR in HCMV-infected cells. Using dCas13 fused to a biotin ligase domain together with a guide RNA (gRNA) specific to the MIE 5' UTR, we identified multiple host and viral proteins that interact with the MIE 5' UTR in infected cells. Several of the identified proteins influenced HCMV replication, both positively and negatively. Further studies confirmed that the cellular YBX1 RNA-binding protein binds to transcripts encoding IE1, IE2, and other HCMV immediate early transcripts in infected cells. Depletion or disruption of YBX1 reduced HCMV replication, which could be rescued by restoring YBX1 expression in trans. YBX1 regulates IE1 and IE2 expression at the posttranscriptional level, as loss of YBX1 expression decreased IE1 and IE2 protein levels despite efficient expression of the UL122 and UL123 transcripts. We found that YBX1 is required for the efficient translation of multiple HCMV immediate mRNAs, as depletion or disruption of YBX1 decreased their association with polysomes, which could be rescued by restoring YBX1 expression. Together, these results reveal a posttranscriptional mechanism controlling the expression of HCMV immediate early gene expression and HCMV replication and provide a sensitive approach for identifying functional RNA:protein interactions in a biologically relevant context.

Materials and Methods

Cells and Viruses. MRC-5, 293T, and HeLa cells were cultured in Dulbecco's Modified Eagle Medium (DMEM, Sigma) supplemented with 10% fetal bovine serum (FBS, Gibco) and penicillin-streptomycin (Sigma) and cultured at 37 °C. Virus stocks were grown on MRC-5 fibroblasts, and titer determined using the 50% tissue culture infectious dose assay ($TCID_{50}$). hTERT-MRC5-DYBX1 cells were routinely passaged in the presence of doxycycline. Cells were plated and infected at confluence for all experiments to control for the impact of YBX1 disruption in cell proliferation. AD*in*GFP (68) or TB40/E (69) was used as the wild-type HCMV as indicated. The HCMV luciferase experiments used HCMV TB40/E expressing luciferase from the UL18 promoter which was gifted from Christine O' Connor (70).

Recombinant CAA virus was made as previously described (67). Briefly, *Escherichia coli* (SW105) isolates containing the AD*in*GFP bacterial artificial chromosome (BAC) were made recombination competent by incubation at 42 °C for 15 min prior to electroporation with a kanamycin-levansucrase (KanSacB) expression cassette with 50 nucleotides flanking the insertion site of the HCMV genome. Oligonucleotides "Full CAA Oligo F" and "Full CAA Oligo R" were annealed and amplified using primers "IE UTR CAA F" and "IE UTR CAA R" (*SI Appendix*, Table S1). The PCR product was electroporated into recombination-competent KanSacB bacteria, and colonies selected on LB + 6% sucrose plates and removal of kanamycin resistance confirmed via replica plating. Colonies were screened for gross recombination by restriction digest and the +500 to −500 nucleotides surrounding the insertion site were PCR amplified using "IE Mutant Seq F" and "IE Mutant Seq R" (*SI Appendix*, Table S1) and sequenced to confirm insertion into the HCMV genome. BAC DNA was Nucleobond purified and electroporated into MRC-5 fibroblasts. Two independent isolates were generated and used in this study.

Lentivirus Transduction. Lentiviruses were made by transfecting 500 ng of DNA per 6-well of HEK293T cells using polyethlyenimine (PEI; Sigma) and MISSION Lentiviral Packaging Mix (Sigma). At 24 h posttransfection, the medium was discarded and replaced with fresh DMEM supplemented with 10% FBS and penicillin-streptomycin. Medium was collected at 48- and 72-h posttransfection, filtered with a 0.45 μM filter, aliquoted, and stored at −80 °C until use. Low-passage cells were transduced with 10 mLs of lentivirus per 15 cm plate of subconfluent MRC-5s using polybrene (hexamethrine bromide, 8 μg/mL) and incubated overnight at 37 °C. The next morning, the lentivirus was aspirated from the cells and replaced with fresh DMEM supplemented with 10% FBS and penicillin-streptomycin. When the cells reached 70% confluency, cells were selected with puromycin. Cells were checked for dPspCas13-TurboID expression and function and kept under puromycin selection until used for experiments. Stable MRC-5 cells expressing dPspCas13-TurboID were transduced with lentivirus for the gRNAs and transduction efficiency determined via fluorescence.

Disruption of YBX1. MRC5 hTERT cells were reverse transfected with Cas9 2NLS nuclease (Synthego) and a pool of gene-specific gRNAs targeting YBX1 (UUUUCCAGCAACGAAGGUUU, UUCAUCAACAGGUGAGCUGC) or a nontargeting scrambled control gRNA using Lipofectamine CRISPRMAX transfection reagent (Invitrogen). Clonal cell lines were generated by seeding transfected cells into 96-well plates at 0.7 cells per well together with wild-type MRC5 cells at 1,000 cells per well. MRC5-hTERT cells express the hygromycin resistance gene. To remove wild-type cells from the coculture, 25 μg/mL Hygromycin (47 μM) was added to the wells at 80 to 90% confluency. YBX1 expression in surviving clonal cell lines was measured by western blot. A PCR fragment spanning the target site was generated using the following primers (FWD: CAGACTCACCCACGTGTGC, REV: AGCTGCAAAACAAAGGCATTCT) and then sequenced by Sanger sequencing (sequencing primer: CAGACTCACCCACGTGTGCG). The ICE CRISPR analysis tool (ice.synthego.com) was used to confirm YBX1 disruption.

Generation of Recombinant Plasmids. PspCas13b and dPspCas13b (PspCas13b-NES-3xHA #103862, dPspCas13b-NES-3xHA #103865), TurboID [C1(1-29)-TurboID-V5_pCDNA3 #107173], and PCW (PCW-Cas9 #50661) plasmids were purchased from Addgene. Both PspCas13b and dPspCas13b plasmids were amplified using primers "PCW-PspCas13b F" and "PspCas13b-Linker R." TurboID was amplified using primers "Linker-TurboID F" and "TurboID-PCW R." PCRs were treated with DpnI for 1 h at 37 °C and PCR purified (QIAquick PCR Purification Kit), and product was run out on a 1% agarose gel to confirm product size. The PCW-Cas9 plasmid was digested with BamHI and NheI, and the 7.5 kb PCW band was gel purified (QIAquick Gel Extraction Kit). Fragments were assembled using Gibson Assembly (NEB; M5510AA). 75 ng of backbone was incubated with 5× molar ratios of each PCR product and 1× Gibson Assembly Mastemix at 50 °C for 1 h. The luciferase reporter vectors were made as previously described (67). Briefly, the WT IE1/2 5' UTR was PCR amplified from template cDNA from HCMV-infected cells using primers "IE UTR pGL3 F" and "IE UTR pGL3 R." The CAA reporter was PCR amplified from the annealed CAA ultramers "Full CAA Oligo F" and "Full CAA Oligo R" using primers "IE UTR pGL3 F" and "IE UTR pGL3 R." The PCR products were cloned into the HindIII and NcoI cut sites of the pGL3-control plasmid (Promega; E1741). For gRNAs, a lentivirus vector was purchased from Addgene (Paw13.lentiguide.mCherry #104375) and PCR amplified with primers "pAW13 F" and "pAW13 R." Multiple gRNAs were designed with a 30 nucleotide sequence to specifically target the MIE 5' UTR or scrambled sequence, ordered as gblocks to contain homology to the amplified lentivirus backbone, and assembled using Gibson Assembly. Colonies were selected and sequenced with "gRNA sequencing primer F" and "gRNA sequencing primer R" to confirm cloning reaction. Cloning reactions were transformed into DH5α competent cells (NEB; C2987I) according to the manufacturer's protocol and all sequences confirmed by Sanger sequencing using primers "gRNA Sequencing primer F" and "gRNA Sequencing primer R." Primer and gBlock sequences used in this study are listed in *SI Appendix*, Table S1.

Luciferase Assays. Luciferase assays were performed as described previously (67). Briefly, HeLas were transfected with 250 ng of PspCas13-TurboID, 250 ng of gRNA, and 50 ng of pGL3 reporter using polyethylenimine (PEI; Sigma). Doxycycline was added to a final concentration of 1 μg/mL at 1 h posttransfection. Samples were lysed in passive lysis buffer (Promega) for 20 min at room temperature at 24 h posttransfection. 8 μL of lysate was incubated with 40 μL of luciferase reagent (Promega) for 2 min at room temperature and read on luminometer

with a 5-s integration (Promega GlowMax Navigator). Luminescence readings were normalized to protein concentration, determined via Bradford assay (VWR; E350–1L). HCMV luciferase assays were performed by infecting MRC-5 cells with HCMV at an MOI of 0.1 and incubated at 37 °C for 72 h. Samples were lysed and read as described above.

Western Blot Analysis. Western blots were performed as described previously (71). Briefly, cells were scraped and pelleted at the time of harvest and resuspended in radioimmunoprecipitation assay buffer (50 mM Tris-HCl [pH 7.4], 150 mM NaCl, 1 mM EDTA, 1% NP-40, 1% sodium deoxycholate) supplemented with protease inhibitor cocktail (Roche cOmplete EDTA-free protease inhibitor cocktail). Cells were lysed on ice for 10 min and centrifuged at 15,000 rpm for 10 min at 4 °C to pellet debris. The supernatant was removed and protein concentration determined via the Bradford Assay (VWR; E350–1L). 6× loading dye was added to samples prior to boiling, and equal amounts of protein were resolved on a 10% SDS–PAGE gel and transferred to PVDF membrane (BioRad TurboBlot). Membranes were blocked in 5% milk (AmericanBio) in TBS-T (20 mM Tris-HCl [pH 6.8], 140 mM NaCl, 0.1% Tween 20) for 1 h at room temperature. Blots were washed with TBS-T and incubated with primary antibodies for 1 h at room temperature (mouse antibodies) or overnight at 4 °C (rabbit antibodies). Blots were washed and developed with appropriate horseradish peroxidase (HRP) conjugated secondary antibody in 1% TBS-T for 1 h at room temperature and washed once more with TBS-T before imaging. Western blots were developed by chemiluminescence using a digital imager (BioRad). Antibodies used in this study were as follows: IE1 [1:1,000 (72)], IE2 [1:500 (73)], UL44 (1:1,000; Virusys), UL99 [1:1,000 (74)], EEF1D (1:1,000, Proteintech), RPS6KB1 (1:1,000, Cell Signaling Technology), TRS1 [1:100 (75)], IRS1 [1:100 (75)], UL38 [1:100 (76)], YBX1 (1 :1,000, Proteintech), β-actin (1:500; SantaCruz), α-rabbitHRP (1:10,000; SeraCare), and α-mouse HRP (1:10,000; SeraCare). Primary mouse antibodies were diluted in 1% BSA in TBS-T while primary rabbit antibodies were diluted in 5% BSA in TBS-T. All experiments were performed in biological triplicate; representative western blots shown.

Nucleic Acid Abundance. RNA was extracted as previously described (61, 77). Briefly, cells were scraped and pelleted and resuspended in Trizol (Ambion) and extracted with chloroform. RNA was precipitated overnight with isopropanol and washed with cold 70% ethanol. RNA pellets were treated with DNAse solution (TURBO DNase free kit, Ambion). Equal amounts of RNA were reverse transcribed according to the manufacturer's protocol (High Capacity cDNA Reverse Transcription Kit, ThermoFisher). The thermocycler parameters for reverse transcription were as follows: 25 °C for 10 min, 37 °C for 120 min, 85 °C for 5 min. qRT-PCR was performed using SYBR Green Select Master Mix (Applied Biosystems) and 0.5 μM of gene-specific primers (*SI Appendix*, Table S1). Absolute quantification of the qPCR data was achieved by comparing CT values to a standard curve generated for each specific pair of primer sets.

Proteomic Analysis MIE 5′ UTR-Associated Factors. MRC-5 cells stably expressing dPspCas13b-TurboID and a gRNA specifically targeting the MIE 5′ UTR were kept under selection with puromycin and seeded at 80% confluency at the time of infection. Doxycycline was added at a final concentration of 1 μg/mL the following morning, and the cells were infected 6 h later with an equivalent number of viral genomes to a WT MOI of 3 for 1 h at 37 °C. After 1 h, the inoculum was replaced with fresh DMEM supplemented with 10% FBS and penicillin-streptomycin and returned to incubate at 37 °C. At 23 hours postinfection (hpi), biotin was added at a concentration of 50 μM, and samples were harvested by scraping at 24 hpi, pelleted, and stored at −80 °C until use. Cells pellets were resuspended in 1 mL of fresh resuspended in radioimmunoprecipitation assay (RIPA) buffer (50 mM Tris-HCl [pH 7.4], 1% NP-40, 0.25% sodium deoxycholate, 150 mM NaCl, 1 mM EDTA [pH 8.0], 2 M urea) supplemented with 1× complete protease inhibitor cocktail (Roche). Cells were lysed on ice for 15 min and then sheared by passing through a 27-gauge needle 5 times. Samples were centrifuged at 4 °C for 10 min to pellet debris and the clarified lysate nutated with Streptavidin T1 Dynabeads (Thermo; 65601) for 3 h at 4 °C. Beads were washed 3 times with RIPA buffer followed by 3 washes with 10 mM Tris HCl (pH 7.8). Beads were resuspended in 50 μL of 10 mM Tris HCl (pH 7.8) for on-bead trypsin digestion as previously described (78). Briefly, after the last wash during affinity purification, beads were resuspended in 100 μL of 50 mM ammonium bicarbonate (pH 8.0). On-bead digestion was carried out overnight at 37 °C with 1 μg trypsin, followed by an additional 3-h incubation the next day with another 1 μg trypsin. Beads were pelleted, and the supernatants collected in fresh tubes. The beads were washed twice with 100 μL LC-MS grade water, and washes were combined with the original supernatants. Samples were acidified with trifluoracetic acid at a final concentration of 2%, dried, desalted using peptide desalting spin columns (Pierce), lyophilized, and stored at −80 °C until further analysis.

LC-MS/MS. Peptides were analyzed by liquid chromatography with tandem mass spectrometry (LC/MS/MS) using an Easy nLc 1200 coupled to a QExactive HF mass spectrometer (Thermo Scientific). Samples were injected onto an Easy Spray PepMap C18 column (75 μm id × 25 cm, 2 μm particle size; Thermo Scientific) and separated over a 2-h gradient method. The separation gradient of 5 to 48% mobile phase B at a flow rate of 250 nL/min, where mobile phase A consisted of 0.1% formic acid in water and mobile phase B was 0.1% formic acid in 80% acetonitrile. The QExactive HF was operated in data-dependent mode, selecting the 15 most intense precursors for subsequent fragmentation. The resolution for the precursor scan (m/z 350 to 1700) was set to 60,000, while the resolution for MS/MS scans was set to 15,000. The normalized collision energy for higher-energy collisional dissociation (HCD) was set to 27%. Peptide matching was set to preferred, and precursors with unknown charge states or those with a charge state of 1 and ≥7 were excluded.

Data Analysis. Raw data files were processed using MaxQuant version 1.6.15.0, and searched against the UniProt human database (containing 20,381 entries, downloaded October 2020) and the UniProt HCMV database (strain AD169, taxID: 10360, containing 190 entries, downloaded May 2021), supplemented with a common contaminants database (245 sequences) using the Andromeda search engine within MaxQuant. Trypsin was set as the enzyme specificity, allowing up to two missed cleavage sites, with methionine oxidation and N-terminal acetylation defined as variable modifications. A 1% false discovery rate was applied for data filtering. Match between runs was enabled (5-min match time window, 20-min alignment window), and a minimum of two unique peptides was required for label-free quantification using the LFQ intensities. Further data processing was carried out using Perseus software (79). Reverse hits and proteins identified by only one unique+razor peptide were removed from the dataset. Proteins with less than 50% valid data were excluded, and missing values were imputed based on a normal distribution within Perseus. Log2 fold change (FC) ratios were calculated using the average Log2 LFQ intensities, and Student's *t* test was performed for each pairwise comparison, with *P*-values calculated. Proteins with *P*-values <0.05 and Log2 FC>1 were considered biological interactors.

siRNA Depletion. Dharmacon Horizon Discovery Cherry-Pick Custom Library Tool was used to purchase small interfering RNAs (siRNAs) specific for genes we identified in the proteomics screen and reverse transfected into MRC-5 cells according to the manufacturer protocol (DharmaFECT reverse transfection of siRNA). Briefly, Lipofectamine RNAiMax Transfection Reagent (Invitrogen) and siRNAs were diluted in Optimem (Gibco) and added to empty wells in a 96-well plate. MRC-5 cells were trypsinized and resuspended in serum-free DMEM and added to the plate on top of the transfection mix and incubated at 37 °C for 72 h. Cells were infected with HCMV-luciferase at a MOI of 0.1, and the cells were returned to incubate at 37 °C for 72 h. Luciferase assays were performed as described above.

YBX1 Knockdown. MRC-5 cells were reverse transfected with ON-TARGETplus Human YBX1 siRNA (Horizon Discovery; L-010213-00-0005) or ON-TARGETplus nontargeting siRNA (Horizon Discovery; D-001810-10-05) using Lipofectamine RNAiMax Transfection Reagent (Invitrogen) according to the manufacturer protocol and incubated at 37 °C for 72 h. Cells were seeded to be 80% confluent at 72 hpi and infected with WT HCMV at an MOI of 3. Knockdown efficiency was determined at the time of infection via western blot analysis.

Immunoprecipitation. MRC-5 cells were infected with WT HCMV at an MOI of 3, harvested by scraping, and cross-linked with 0.3% methanol-free formaldehyde (Pierce) in PBS for 30 min at 4 °C. The reaction was quenched with 1/10 volume of 2 M glycine with agitation for 5 min at room temperature. Cell pellets were washed 3 times with cold PBS and resuspended in RIPA-IP buffer (50 mM Tris HCl [pH 8.0], 1% Triton X-100, 0.5% sodium deoxycholate, 0.1% SDS, 5 mM EDTA, 150 mM KCl, 100 mM DTT) with 1× complete protease inhibitor cocktail (Roche)

and SUPERaseIN (Promega). Cells were sonicated with the following parameters: 2× 30 s on, 1 min off, 30% output, and centrifuged at 15,000 rcf for 15 min at 4 °C. A portion of the lysate was reserved to measure input protein levels, and the rest of the supernatant was incubated with Protein A/G PLUS agarose beads (Santa Cruz) for 1 h at 4 °C to remove nonspecific interactions. Protein A/G PLUS beads were washed 3 times with RIPA buffer (50 mM Tris-HCl [pH 7.5], 140 mM NaCl, 1 mM EDTA [pH 8.0], 1 mM EGTA [pH 8.0], 1% Triton X-100, 0.1% sodium deoxycholate, 0.1% SDS, 1× complete protease inhibitor cocktail [Roche]) prior to use. The agarose beads were then removed by low-speed centrifugation, and 5 μg of antibody specific for YBX1 (Proteintech, 20339-1-AP) or rabbit IgG (Cell Signaling Technology, 2729) was added to the supernatant and nutated for 1 h at 4 °C. Protein A/G PLUS beads were then added and the samples were nutated for additional 1 h at 4 °C. Samples were centrifuged for 1 min at 1,200 rcf at 4 °C to pellet beads and washed with the following parameters: 1× with RIPA buffer, 3× with Pol II ChIP buffer (50 mM Tris-HCl [pH 7.5], 140 mM NaCl, 1 mM EDTA, 1 mM EGTA, 1% Triton X-100, 0.1% sodium deoxycholate, and 0.1% SDS), 2× with CLiP Salt Buffer (50 mM Tris-HCl [pH 7.4], 500 mM NaCl, 1 mM EDTA, 1% NP-40, 0.5% sodium deoxycholate, and 0.1% SDS), and 1× with LiCl wash buffer (20 mM Tris-HcL [pH 8.0], 1 mM EDTA, 250 mM LiCl, 0.5% NP-40, and 0.5% sodium deoxycholate). The supernatant was removed after the final wash and the beads resuspended in reverse crosslinking buffer (1× PBS, 2% N-lauroyl sarcosine, 10 mM EDTA [pH 8.0], 4 mM DTT, proteinase K, SUPERaseIN [Promega]) and incubated for 1 h at 42 °C, 1 h at 55 °C, and 30 min at 65 °C with mixing every 15 min. RNA was extracted from samples with Trizol according to the protocol above. Fold enrichment was calculated using the comparative C_t method of YBX1 signal versus IgG, normalized to the level of *GAPDH* mRNA in each sample.

Translation Efficiency Analysis. Polysome analysis was performed as previously described (61, 67, 77, 80). Briefly, cells were treated with 100 μg/mL cycloheximide at the time of harvest and incubated at 37 °C for 10 min. Cells were washed with PBS containing cycloheximide, harvested by scraping, and pelleted by centrifugation at 2,200 rpm for 5 min at 4 °C. Pellets were stored at −80 °C until analysis. Pellets were lysed in polysome lysis buffer (20 mM Tris-HCl [pH 7.4], 140 mM KCl, 5 mM $MgCl_2$, 0.1% Triton X-100, and 10 mM DTT) and sheared by passaging through a 27-gauge needle 5 times. Samples were centrifuged for 5 min at 2,500 rcf at 4 °C to pellet the nuclei followed by centrifugation for 10 min at 13,000 rcf at 4 °C to pellet the mitochondria. Protein concentration was determined via Bradford assay (VWR), and equal amounts of protein were loaded onto a 10 to 15% linear sucrose gradient. Gradients were centrifuged at 35,000 rpm for 2 h without brake, and then fractionated with continuous monitoring of UV absorbance at 254 nm. RNA was extracted from equal volumes of gradient fractions with Trizol as previously mentioned, and equal volumes of RNA were added into the RT reaction. RNA abundance in each fraction was determined by qRT-PCR using the absolute quantification method. Translation efficiency was calculated by comparing the abundance of transcripts associated with polysomes (fractions 7 to 12) and monosomes (fractions 2 to 5).

HCMV Replication Assays. MRC-5 primary fibroblasts were infected with HCMV at an MOI of 3 for 1 h at 37 °C with rocking every 15 min. The inoculum was then removed and replaced with fresh medium until the time of harvest. Supernatants were collected and stored at −80 °C until analysis. Cell-free infectious virus in the supernatants was quantified via the $TCID_{50}$ assay.

Results

Identification of Proteins Proximal to the MIE 5' UTR in HCMV-Infected Cells. For many transcripts, the 5' UTR serves as a binding site for factors that influence ribosome recruitment and subsequent translation. To better understand factors involved in the posttranscriptional regulation of IE1 and IE2 expression, we developed a system to identify proteins in close proximity to the MIE 5' UTR in infected cells. We took advantage of the fact Cas13 can be programmed to bind to a specific RNA target in the presence of a gRNA complementary to the target site. Catalytically inactive Cas13 variants lose their ability to cleave nucleic acid targets while retaining the ability to bind to a specific RNA sequence in complex with a gRNA. While several Cas13 orthologs exist, Cas13b from *Prevotella sp. P5-125* (PspCas13b) was selected for its increased stability in mammalian cells and target specificity due to its relatively long gRNA spacer sequence compared to other Cas13 orthologs (81–83). We took advantage of these features of PspCas13b to develop a proteomics approach to identify proteins that associate with specific RNA elements.

We designed a catalytically inactive PspCas13b protein fused to a biotin ligase domain (dPspCas13b-TurboID) under the control of a doxycycline-inducible promoter, allowing for controlled PspCas13b expression. We hypothesized that in the presence of a specific gRNA (Fig. 1*A*), dPspCas13b-TurboID would localize to a specific RNA sequence, allowing the biotin ligase to covalently modify proteins in close proximity [within 10 nM; (84)] with biotin. The biotinylated proteins would then be captured with streptavidin beads and identified via mass spectrometry. To avoid potential steric hindrances that might affect dPspCas13b or TurboID function, a flexible linker was included between the two domains. The dPspCas13b-TurboID fusion protein retained biotin ligase activity in transfected cells, as shown by the nonspecific increase in the abundance of biotinylated proteins in cells expressing dPspCas13b-TurboID in the absence of a specific gRNA (Fig. 1*B*). To determine whether the presence of the TurboID domain affected PspCas13b function, we designed and tested the ability of gRNAs to specifically target PspCas13b to the MIE 5' UTR. Cells were transfected with a catalytically active PspCas13b-TurboID expression construct along with gRNAs complementary to the MIE 5' UTR and a vector expressing the MIE 5' UTR upstream of a luciferase reporter. Catalytically active PspCas13b-TurboID was used in these experiments, as specific targeting of the active enzyme to an mRNA should decrease its abundance without affecting other mRNAs. Of 10 gRNAs tested, six significantly reduced the luciferase signal of the MIE reporter and did not affect the activity of a control reporter gene where the 5' UTR consisted of a series of CAA repeats (Fig. 1*C*). These results demonstrate that a PspCas13-TurboID fusion protein retains biotin ligase activity and the ability to target a specific RNA. gRNA 4 was used in subsequent experiments due to its ability to specifically target the MIE 5' UTR.

We next used lentivirus transduction to generate a human fibroblast cell line expressing dPspCas13b-TurboID under the control of a doxycycline-inducible promoter (MRC5-dPspCas13b-TurboID) together with a gRNA specific for the MIE 5' UTR. To identify proteins that are proximal to the MIE 5' UTR during infection, cells were treated with doxycycline to induce dPspCas13b-TurboID expression prior to infection, and then infected with either wild-type HCMV or a previously described recombinant HCMV in which the MIE 5' UTR sequence is replaced with CAA repeats [CAA HCMV; (67, 85)] as a control for specificity. Biotin was added 1 h prior to harvest at 24 h hpi to allow for proximity labeling, and the labeled proteins were recovered by streptavidin immunoprecipitation and identified by mass spectrometry. Multiple proteins were significantly enriched in samples infected with wild-type virus as compared to the control, suggesting our approach specifically captured proteins associated with the MIE 5' UTR [Fig. 2*A* and *SI Appendix*, Table S2; (86)].

Analysis of the annotated function of enriched proteins revealed that many of the factors were RNA-binding proteins with known roles across the RNA lifecycle (Fig. 2*B*). Interestingly several known HCMV RNA-binding proteins were identified [e.g., UL69, UL84; (87–90)], suggesting a potential functional role for these proteins in regulating RNA biology during infection (*SI Appendix*, Table S2). Based on these results we chose 38 proteins for further analysis. We used siRNAs to deplete each factor from human fibroblasts, and then measured the effect on luciferase expression from an HCMV reporter virus encoding the luciferase

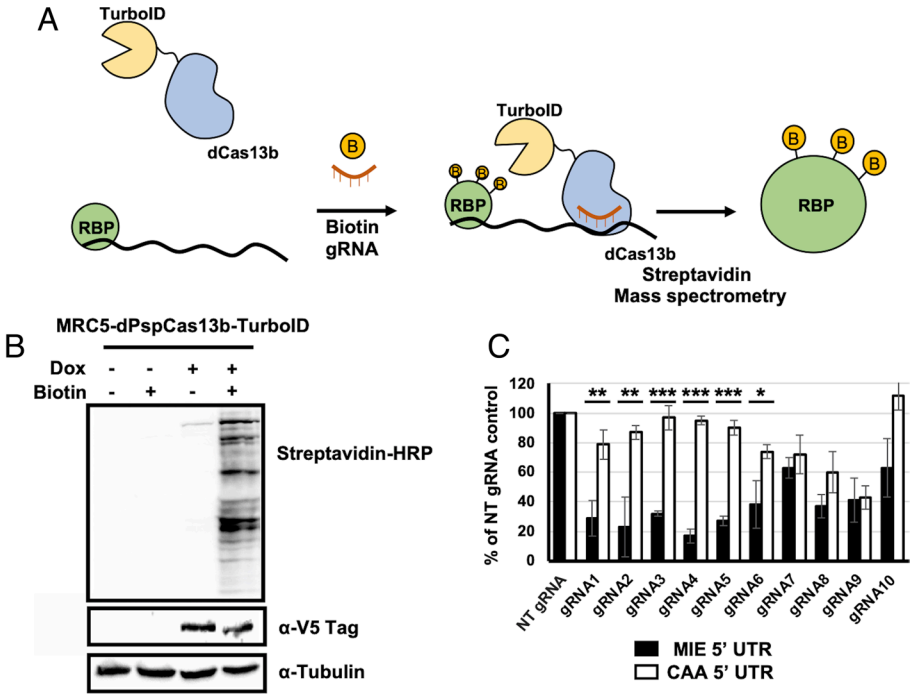

Fig. 1. dCas13b-TurboID can specifically target the MIE 5′ UTR. (*A*) Catalytically inactive PspCas13b (dPspCas13b, blue) is fused with a biotin ligase domain (TurboID; yellow) via a flexible linker. In the presence of biotin (*B*, gold), and a gRNA specific to the RNA of interest, PspdCas13b targets TurboID to a specific location on the RNA. TurboID then covalently labels proximal proteins (RBP: RNA-binding protein, green), which are immunoprecipitated and identified via mass spectrometry. (*B*) dCas13b-TurboID expression and biotin ligase activity were measured in MRC5 fibroblasts expressing dCas13b-TurboID (MRC5-dCas13b-TurboID). (*C*) HeLa cells were transfected with active Cas13b, together with gRNAs specific for the MIE 5′ UTR, and a luciferase reporter vector containing either the MIE 5′ UTR sequence (black bars) or a series of CAA repeats upstream of the luciferase gene (white bars). Luciferase results were compared to a scrambled sequence (NT gRNA). (n = 3 ± SEM, **P* < 0.05, ***P* < 0.01, ****P* < 0.001).

gene under the control of the UL18 late promoter (70) and compared the results to control cells transfected with a nonspecific siRNA control. In this system, luciferase activity serves as a measure of HCMV replication, as UL18 promoter activity requires prior genome replication. Transfection of siRNAs targeting the cellular ERH, FAM120A, GEMIN5, HNRNPH2, IGF2BP1, IGF2BP3, KHDRBS1, NONO, RNPS1, RPL35, RPL5, SNRPD1, UPF1, YES1, and ZNF207 genes increased luciferase activity, suggesting a potential role for these factors in suppressing HCMV replication. Transfection of siRNAs targeting six other genes (EIF2S3, EIF4A3, HNRNPA0, PRMT1, PTBP1, and YBX1) led to a significant decrease in luciferase activity as compared to control cells, suggesting a requirement for these factors for efficient HCMV replication (Fig. 2*C*). While enrichment in the proteomics screen and altered replication in the siRNA screen suggest important roles for these factors in HCMV infection, the results should be interpreted with caution without further studies to confirm viral RNA binding and the specificity of observed replication phenotypes. However, these results identify cellular and viral genes of interest for further study in the regulation of RNA biology during infection and suggest that host factors in close proximity to the MIE 5' UTR in infected cells regulate HCMV replication.

YBX1 Is Critical for Efficient HCMV Replication. Based on the defect in luciferase activity when YBX1 was depleted, we further explored the role of YBX1 in HCMV infection. Using immunoprecipitation with antibodies specific for YBX1 and quantitative reverse transcriptase PCR (qRT-PCR), we next measured the association of YBX1 with transcripts encoding HCMV immediate early mRNAs. Transcripts encoding five immediate early RNAs (*UL38*, *TRS1*, *IRS1*, *UL122*, and *UL123*) were significantly enriched in YBX1-specific immune precipitates compared to a nonspecific IgG at 24 h (Fig. 3*A*) after infection. The EEF1D and RPS6KB1 transcripts were used as positive and negative controls for YBX1 binding, respectively, based on a previous report (91).

We next measured the effect of YBX1 gene disruption on the expression of viral proteins and the yield of infectious virus. We used CRISPR-Cas9 to generate MRC-5 cells where the YBX1 gene was disrupted leading to loss of YBX1 protein expression (hTERT-MRC5-ΔYBX1 cells). In parallel, we generated control cells expressing a nonspecific gRNA (hTERT-MRC5-NT). To allow for controlled reexpression of YBX1, we transduced hTERT-MRC5-ΔYBX1 cells with a lentivirus expressing YBX1 under the control of a doxycycline-inducible promoter, allowing for restored YBX1 expression in the presence of doxycycline. YBX1 disruption reduced cell proliferation, which was rescued by the addition of doxycycline to restore YBX1 expression (*SI Appendix*, Fig. S1). To control for the effect on proliferation, all experiments were performed using fully confluent cultures. To measure the impact of YBX1 HCMV entry and initial viral transcription, we measured the abundance of intracellular viral genomes and transcripts encoding IE1 or IE2 at 24 h after infection. Depletion of YBX1 did not impact intracellular HCMV genome abundance or the abundance of transcripts encoding IE1 and IE2 (Fig. 3 *B* and *C*, respectively), demonstrating that YBX1 was dispensable for HCMV binding, entry, and initial transcription from the viral genome. Similar results were seen after infection with the HCMV TB40/E strain (*SI Appendix*, Fig. S2), which is more closely related to clinical viral isolates. Despite similar IE1 and IE2 transcript levels, IE1 and IE2 protein levels were decreased at early times (6 and 24 hpi) after infection in the absence of YBX1 (Fig. 3*D*). We also observed delayed and reduced expression of representative HCMV early and late proteins in the absence of YBX1, consistent with the known role of IE1 and IE2 in positively regulating early

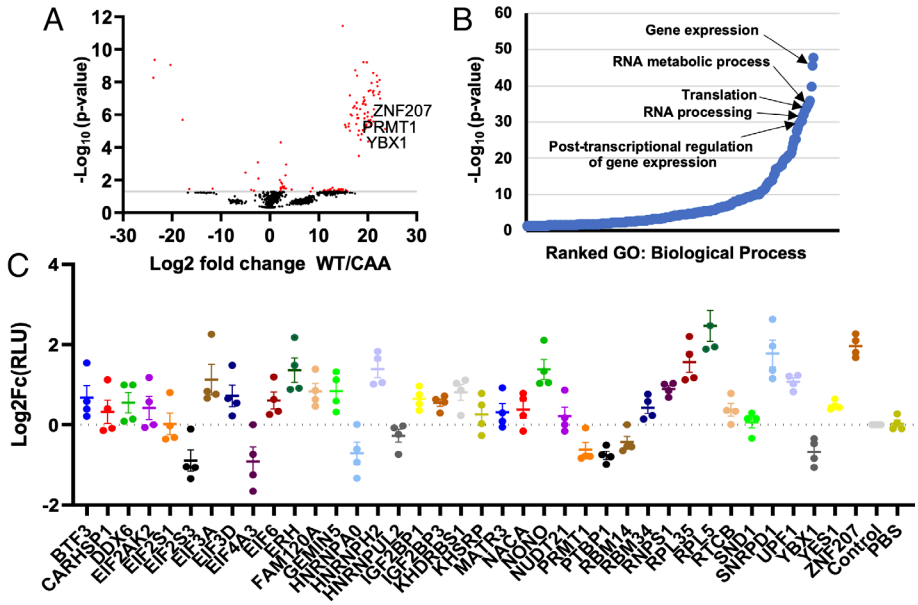

Fig. 2. Multiple proteins associated with the MIE 5′ UTR regulate HCMV replication. (*A*) MRC5-dCas13b-TurboID cells expressing a gRNA specific to the MIE 5′ UTR were infected with either WT virus or CAA recombinant virus with equivalent genomes equal to an MOI of 3 for WT virus. Volcano plot showing the proteomics data from three independent replicates (Red = statistically significant). (*B*) Gene ontology (GO) analysis of the biological processes of proteins identified in (*A*). (*C*) MRC5 cells were transfected with the indicated siRNA prior to infection with HCMV TB40/E expressing luciferase under the control of the UL18 late promoter at an MOI of 0.1. The luciferase assay was read and at 72 h after infection. The Log2Fold change in luciferase activity compared to cells transfected with a nonspecific control siRNA. The results of four individual wells from two independent experiments are shown.

and late gene expression. Consistent with the defect in viral protein expression, significantly less infectious virus was produced in hTERT-MRC5-ΔYBX1 cells as compared to the hTERT-MRC5-NT control cells (Fig. 3*E*). Similar results were seen when shRNAs were used to deplete YBX1 prior to infection (*SI Appendix*, Fig. S3). Depleting YBX1 prior to infection reduced IE1 and IE2 expression without affecting transcript levels and delayed and reduced viral protein expression and the accumulation of infectious virus. Importantly, restoring YBX1 expression by adding doxycycline to hTERT-MRC5-ΔYBX1 cells prior to infection rescued the defect in viral gene expression and restored virus yield to levels similar to those observed in control cells (Fig. 3 *D* and *E*), demonstrating that the defect in HCMV protein expression and replication in hTERT-MRC5-ΔYBX1 was specific to the absence of YBX1. Together, these data show that YBX1 is critical for efficient IE1 and IE2 expression early after infection, and that reduced IE1 and IE2 expression likely accounts for the decrease in early and late gene expression and virus yield when YBX1 is absent.

YBX1 Is Required for the Efficient Translation of HCMV Immediate Early RNAs. YBX1 regulates the translation of a subset of cellular mRNAs associated with cell proliferation, apoptosis, DNA repair, and stress response and the antiviral response by binding to their 5′ UTRs (92–101). In addition, some viruses exploit YBX1 to enhance viral mRNA translation (102–106). The defect in viral protein expression and virus replication suggested that YBX1 may similarly regulate the translation of HCMV RNAs. To determine the role of YBX1 in viral mRNA translation, we measured the impact of YBX1 disruption on the association of viral RNAs with polysomes. Control cells or hTERT-MRC5-ΔYBX1 cells were infected with HCMV for 24 h, and ribosomal subunits, individual ribosomes, and polysomes were resolved through a sucrose gradient, and the distribution of viral RNAs across the gradient was measured by qRT-PCR. Transcripts encoding the HCMV *IE1* or *TRS1* proteins were less abundant in fractions containing polysomes in hTERT-MRC5-ΔYBX1 cells as compared to control cells with a corresponding increase in transcript abundance in earlier fractions of the gradient containing ribosomal subunits and individual ribosomes (Fig. 4*A*). The distribution of the negative control *RPS6KB1* mRNA was similar in all conditions. Similar to the viral transcripts, the positive control EEF1D transcript was less abundant in polysomes in the absence of YBX1. Restoring YBX1 expression prior to infection increased the abundance of each viral transcript and the EEF1D transcript in polysome fractions to similar levels as in control cells, demonstrating that the change in polysome association was dependent on the presence of YBX1 (Fig. 4*A*).

We used these data to calculate the translation efficiency of each transcript in the presence and absence of YBX1 by comparing the abundance of each RNA in fraction containing polysomes to its abundance in fractions containing ribosomal subunits and individual ribosomes. Loss of YBX1 expression led to a significant decrease in the translation efficiency of transcripts encoding IE1, IE2, UL38, TRS1, IRS1, and the EEF1D positive control without affecting the translation efficiency of the RPS6KB negative control (Fig. 4*B*). In each case, the decrease in translation efficiency in the absence of YBX1 resulted in a corresponding decrease in protein expression (Fig. 4*C*). Similar results were observed for transcripts encoding IE1 and IE2 at 6 h after infection in cells where YBX1 had been depleted prior to infection using specific shRNAs. YBX1 depletion decreased the abundance of transcripts encoding IE1 and IE2 in fractions containing polysomes, with a corresponding increase in transcript abundance in earlier gradient fractions containing ribosomal subunits and monosomes as compared to control cells (*SI Appendix*, Fig. S4*A*). YBX1 depletion significantly reduced the translation efficiency of transcripts encoding both IE1 and IE2 at 6 h as compared to control cells with no significant impacts on the translation efficiency of the cellular *GAPDH* mRNA (*SI Appendix*, Fig. S2*B*). Together with the data from YBX1 knockout cells, these data support the conclusion that YBX1 enhances virus replication by facilitating the translation of mRNAs encoding HCMV immediate early genes.

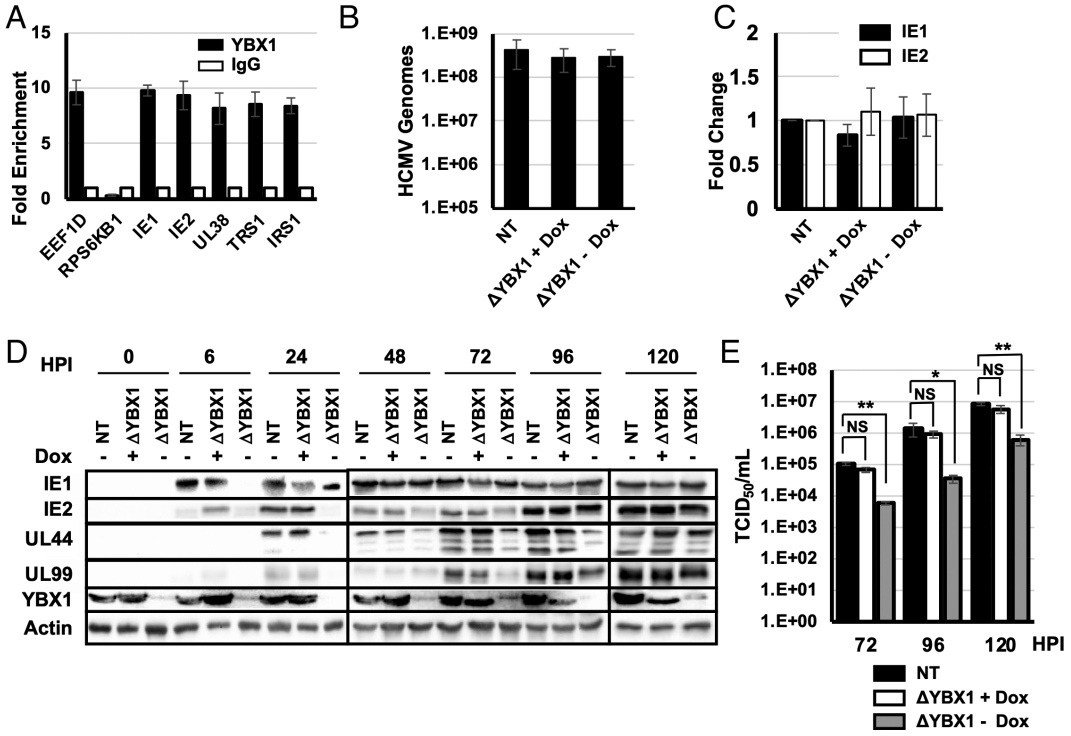

Fig. 3. YBX1 rescue restores HCMV replication. (*A*) MRC5 cells were infected at an MOI of 3 and cross-linked with formaldehyde at 24 hpi for immunoprecipitation with a YBX1 antibody (black) or species-matched IgG control antibody (white). RNA from immune precipitates was purified and analyzed via qRT-PCR. EEF1D was used as a positive control and RPS6KB1 was used as a negative control for YBX1 binding. Enrichment was calculated using the comparative C_t method of YBX1 signal versus IgG. (*B*) Confluent monolayers of cells expressing a nonspecific gRNA (NT- hTERT-MRC5-NT) or hTERT-MRC5-ΔYBX1 cells were infected with HCMV at an MOI of 3 in the presence (DYBX1+Dox) or absence (DYBX1) of doxycycline and intracellular genomes were quantified at 24 hpi. (*C*–*E*) Cells were infected as in (*B*), and (*C*) IE1 and IE2 transcript abundance was measured by qRT-PCR at 24 hpi, and (*D*) the expression of representative immediate early (IE1, IE2), early (UL44), and late (UL99) viral proteins was measured by western blot at the indicated times after infection. Representative results from three independent experiments are shown. (*E*) Cell-free virus was measured at 72, 96, and 120 h after infection using the $TCID_{50}$ method. (Black bars = NT cells; white bars = hTERT-MRC5-ΔYBX1 with doxycycline; gray bars = hTERT-MRC5-ΔYBX1 without doxycycline; $n = 3 \pm$ SEM, $^*P < 0.05$, $^{**}P < 0.01$, NS = not significant).

Discussion

To identify potential regulators of HCMV mRNA translation, we developed a proteomics approach to identify proteins in close proximity to a target RNA in its normal physiological context inside the cell. Using this approach, we identified potential cellular and viral proteins associated with the 5' UTR of transcripts encoding the IE1 and IE2 proteins in HCMV-infected cells. We confirmed that one interactor, YBX1, binds mature transcripts encoding IE1 and IE2 and positively regulates the translation of multiple HCMV immediate early genes. YBX1 was necessary for the efficient expression of HCMV immediate early, early, and late proteins and the production of infectious virions, demonstrating a critical role for YBX1 in HCMV gene expression and replication.

Defining the complement of proteins associated with a specific RNA provides a powerful system to identify factors that regulate gene expression at the posttranscriptional level. Our approach addresses several complications arising from the more traditional approach of incubating in vitro transcribed labeled RNAs bait with cell lysates, followed by mass spectrometry to identify associated factors. While useful, this approach has several limitations, including requiring supraphysiological levels of "bait" RNA, the potential for false positive interactions with the affinity tag, and the presence of spurious interactions that would not occur in the spatial constraints of an intact cell. The approach described here overcomes these challenges by identifying potential interactions using the endogenous RNA expressed under the control of its native promoter. This approach should be generally applicable for identifying RNA:protein interactions for any given RNAs that can be specifically targeted by a gRNA but may be especially useful for studying dynamic changes in RNA:protein interactions that occur inside a cell in response to cellular stressors such as viral infection.

Our proteomics screen identified multiple cellular and viral proteins likely associated with transcripts encoding IE1 and IE2 (*SI Appendix*, Table S2). Several identified HCMV proteins have defined roles in RNA biology during infection [e.g., pTRS1, UL69; (88, 89, 107–111)], while others such as UL29 and UL112/113 have not previously been reported to bind nucleic acids. These data could suggest a potential role for these factors in regulating HCMV gene expression at a posttranscriptional level. Similarly, many of the cellular factors identified in the screen are known regulators of RNA biology or metabolism, suggesting a role in RNA biology during infection. Interestingly siRNA's targeting several of the enriched cellular proteins enhanced HCMV replication, implicating these factors in the host antiviral response. In contrast, siRNAs targeting several other cellular genes decreased HCMV replication. Two such genes, EIF4A3 and YBX1, regulate HCMV gene expression at a posttranscriptional level [Fig. 4 and (112)], potentially suggesting similar roles for other factors required for virus replication. While enrichment in the proteomics screen and altered replication in the siRNA screen suggest important roles in HCMV infection, these results should be interpreted with caution without further studies to confirm viral RNA binding and the specificity of the observed replication phenotypes. However, these cellular and viral genes may be of interest for

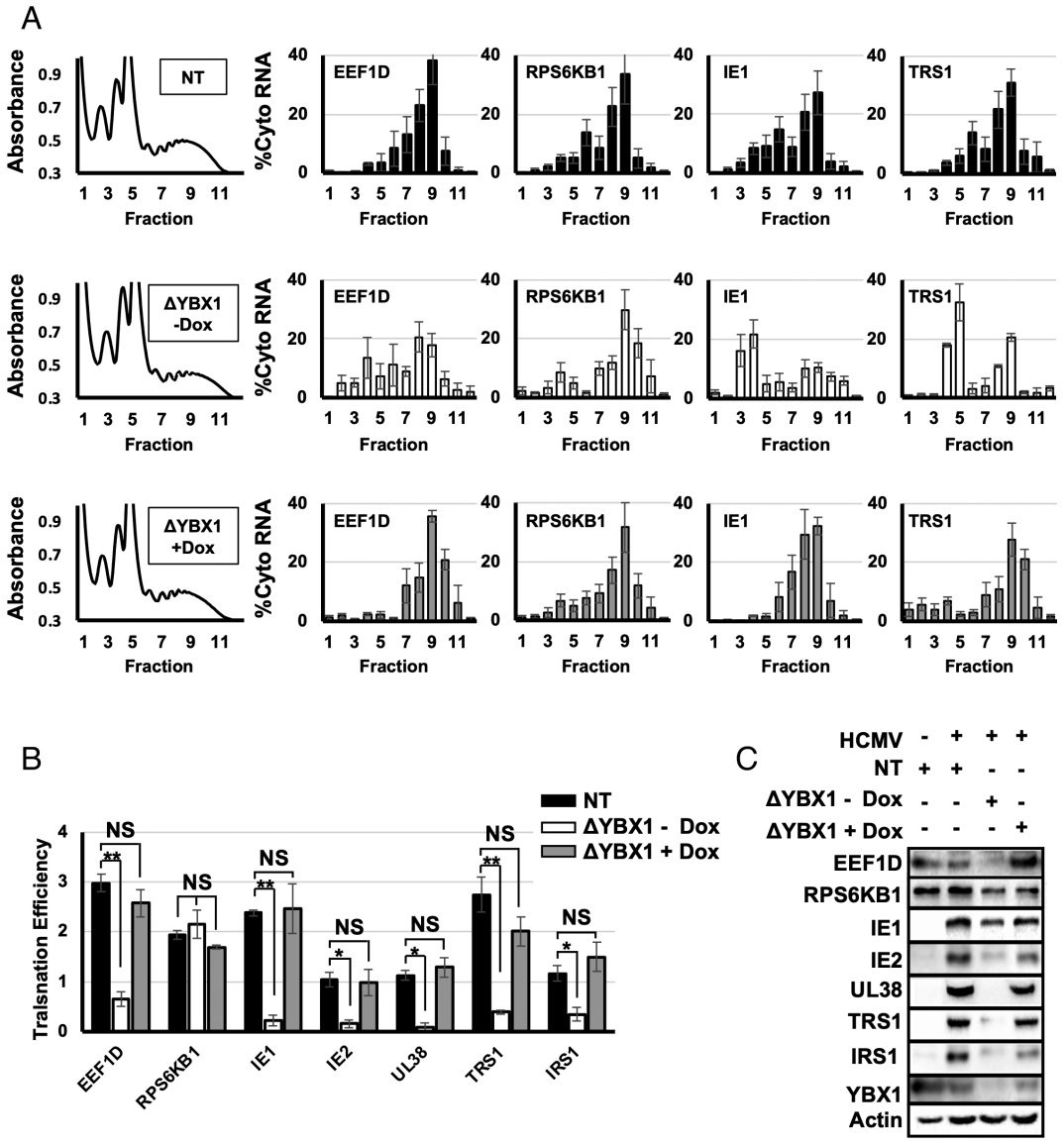

Fig. 4. YBX1 regulates translation of HCMV immediate early transcripts. (*A*) CRISPR was used on hTERT-MRC5 fibroblasts to generate either a control cell line (NT, black) or a YBX1-depleted cell line (ΔYBX1 −Dox, white). YBX1 was recovered in knockdown cells with a lentivirus expressing YBX1 under a dox inducible promoter (ΔYBX1 +Dox, gray). Cells were infected with HCMV at an MOI of 3 and harvested at 24 hpi. Cytoplasmic lysates resolved over a 10 to 50% linear sucrose gradient and RNA analyzed via qRT-PCR. (*B*) Translation efficiency was calculated by comparing the abundance of RNA transcripts with polysomes to monosomes. (*C*) Cells were infected as in (*B*) and harvested for protein analysis via western blot. ($n = 3 \pm$ SEM, $^*P < 0.05$, $^{**}P < 0.01$).

further study in the regulation of RNA biology during infection, and suggest that host factors in close proximity to the MIE 5' UTR in infected cells regulate HCMV replication.

Using this approach, we identified YBX1 as a cellular factor that binds to viral immediate early transcripts. An interesting question arising from this work is the nature of YBX1 recognition of HCMV mRNAs. YBX1 typically binds to the 5' and 3' untranslated regions of mRNAs, recognizing specific sequences and secondary structures (93, 100, 113–116). The 5' UTR of mature transcripts encoding IE1 and IE2 contain specific RNA structures that enhance the translation of IE1 and IE2 encoding transcripts during infection (85). Perhaps these structures serve as YBX1-binding sites. However, mRNAs encoding the other HCMV immediate early genes have unique 5' UTRs and do not share obvious sequence homology but could potentially contain similar RNA structures that are recognized by YBX1. Alternatively, YBX1 could recognize HCMV RNAs as a result of their high GC content or the potential presence of 5' methylcytosine modifications, both common features of cellular YBX1 cognate RNAs (95, 102). Additional studies to discriminate between these possibilities and others will be needed to define the sequences, modifications, and/or RNA structures that YBX1 may recognize in viral RNAs.

Our data show that YBX1 is required for the efficient translation of multiple HCMV immediate early transcripts. While often considered a translational repressor, YBX1 enhances the translation of a specific subset of cellular mRNAs (117). For example, YBX1 enhances the translation of mRNAs encoding factors involved in stress response and proliferation (114, 115, 118), and some viruses exploit YBX1 to enhance viral mRNA translation (102–106). Interestingly, YBX1 also promotes the translation of specific mRNAs under conditions that impair cap-dependent translation and also enhances the translation of mRNAs with internal ribosome entry sites (IRES) activity (117). We previously found that HCMV immediate early mRNA translation is resistant to disruption of the canonical eIF4F translation initiation complex (77), and viral late protein synthesis proceeds

unabated despite activation of the integrated stress response, which severely disrupts protein synthesis in uninfected cells (119). A model consistent with our data would be that YBX1 binds specific sequences or structures in HCMV mRNAs and facilitates ribosome recruitment, perhaps independently of eIF4F, to enhance viral immediate early protein expression or maintain viral protein synthesis in the face of the cellular stress response. Future studies to define the molecular mechanisms(s) by which YBX1 enhances viral protein synthesis will be needed to explore these possibilities.

Data, Materials, and Software Availability. Mass spectrometry data have been deposited to the ProteomeXchange Consortium (http://proteomecentral.proteomexchange.org) via the PRIDE partner repository with the dataset identifier PDX054962 (86).

ACKNOWLEDGMENTS. We wish to acknowledge members of the Moorman lab for helpful conversations and discussions. This study was supported by grants R01-AI103311 and R21-AI123811 to N.J.M. from the NIH, and the University of North Carolina Cancer Research Fund, and National Cancer Institute Center Core Support Grant (2P30CA016086-45) to the University of North Carolina Lineberger Comprehensive Cancer Center.

1. M. Zuhair *et al.*, Estimation of the worldwide seroprevalence of cytomegalovirus: A systematic review and meta-analysis. *Rev. Med. Virol.* **29**, e2034 (2019).
2. H. Buxmann, K. Hamprecht, M. Meyer-Wittkopf, K. Friese, Primary human cytomegalovirus (HCMV) infection in pregnancy. *Dtsch. Arztebl. Int.* **114**, 45–52 (2017).
3. M. J. Cannon, K. F. Davis, Washing our hands of the congenital cytomegalovirus disease epidemic. *BMC Public Health* **5**, 70 (2005).
4. L. Pembrey *et al.*, Seroprevalence of cytomegalovirus, Epstein Barr virus and varicella zoster virus among pregnant women in Bradford: A cohort study. *PLoS One* **8**, e81881 (2013).
5. P. Griffiths, M. Reeves, Pathogenesis of human cytomegalovirus in the immunocompromised host. *Nat. Rev. Microbiol.* **19**, 759–773 (2021).
6. S. F. Atabani *et al.*, Cytomegalovirus replication kinetics in solid organ transplant recipients managed by preemptive therapy. *Am. J. Transplant.* **12**, 2457–2464 (2012).
7. M. Boeckh, W. G. Nichols, The impact of cytomegalovirus serostatus of donor and recipient before hematopoietic stem cell transplantation in the era of antiviral prophylaxis and preemptive therapy. *Blood* **103**, 2003–2008 (2004).
8. J. R. Deayton *et al.*, Importance of cytomegalovirus viraemia in risk of disease progression and death in HIV-infected patients receiving highly active antiretroviral therapy. *Lancet* **363**, 2116–2121 (2004).
9. X. Cui, C. M. Snapper, Development of novel vaccines against human cytomegalovirus. *Hum. Vaccin. Immunother.* **15**, 2673–2683 (2019).
10. S. Scarpini *et al.*, Development of a vaccine against human cytomegalovirus: Advances, barriers, and implications for the clinical practice. *Vaccines (Basel)* **9**, 551 (2021).
11. C. S. Nelson, B. C. Herold, S. R. Permar, A new era in cytomegalovirus vaccinology: Considerations for rational design of next-generation vaccines to prevent congenital cytomegalovirus infection. *NPJ Vaccines* **3**, 1–9 (2018).
12. D. J. Diamond *et al.*, A fifty-year odyssey: Prospects for a cytomegalovirus vaccine in transplant and congenital infection. *Expert Rev. Vaccines* **17**, 889–911 (2018).
13. S. A. Plotkin, S. B. Boppana, Vaccination against the human cytomegalovirus. *Vaccine* **37**, 7437–7442 (2019).
14. T.-M. Fu, Z. An, D. Wang, Progress on pursuit of human cytomegalovirus vaccines for prevention of congenital infection and disease. *Vaccine* **32**, 2525–2533 (2014).
15. A. E. Lilja, P. W. Mason, The next generation recombinant human cytomegalovirus vaccine candidates–Beyond gB. *Vaccine* **30**, 6980–6990 (2012).
16. K. C. Arnold, C. J. Flint, Cytomegalovirus, parvovirus B19, varicella zoster, and toxoplasmosis in pregnancy. *Obstet. Gynecol.* **125**, 1510 (2015).
17. S. P. Walker, R. Palma-Dias, E. M. Wood, P. Shekleton, M. L. Giles, Cytomegalovirus in pregnancy: To screen or not to screen. *BMC Pregnancy Childbirth* **13**, 96 (2013).
18. W. J. Britt, M. N. Prichard, New therapies for human cytomegalovirus infections. *Antiviral Res.* **159**, 153–174 (2018).
19. K. B. Fowler, S. B. Boppana, Congenital cytomegalovirus infection. *Semin. Perinatol.* **42**, 149–154 (2018).
20. G. El Helou, R. R. Razonable, Safety considerations with current and emerging antiviral therapies for cytomegalovirus infection in transplantation. *Expert Opin. Drug Saf.* **18**, 1017–1030 (2019).
21. R. R. Razonable, Drug-resistant cytomegalovirus: Clinical implications of specific mutations. *Curr. Opin. Organ Transplant.* **23**, 388–394 (2018).
22. M. Chevillotte *et al.*, A new tool linking human cytomegalovirus drug resistance mutations to resistance phenotypes. *Antiviral Res.* **85**, 318–327 (2010).
23. B. Rozman *et al.*, Temporal dynamics of HCMV gene expression in lytic and latent infections. *Cell Rep.* **39**, 110653 (2022).
24. F. S. Leach, E. S. Mocarski, Regulation of cytomegalovirus late-gene expression: Differential use of three start sites in the transcriptional activation of ICP36 gene expression. *J. Virol.* **63**, 1783–1791 (1989).
25. M. F. Stinski, D. R. Thomsen, R. M. Stenberg, L. C. Goldstein, Organization and expression of the immediate early genes of human cytomegalovirus. *J. Virol.* **46**, 1–14 (1983).
26. A. Marchini, H. Liu, H. Zhu, Human cytomegalovirus with IE-2 (UL122) deleted fails to express early lytic genes. *J. Virol.* **75**, 1870–1878 (2001).
27. W. Dunn *et al.*, Functional profiling of a human cytomegalovirus genome. *Proc. Natl. Acad. Sci. U.S.A.* **100**, 14223–14228 (2003).
28. R. F. Greaves, E. S. Mocarski, Defective growth correlates with reduced accumulation of a viral DNA replication protein after low-multiplicity infection by a human cytomegalovirus ie1 mutant. *J. Virol.* **72**, 366–379 (1998).
29. M. Nevels, C. Paulus, T. Shenk, Human cytomegalovirus immediate-early 1 protein facilitates viral replication by antagonizing histone deacetylation. *Proc. Natl. Acad. Sci. U.S.A.* **101**, 17234–17239 (2004).
30. C. Paulus, S. Krauss, M. Nevels, A human cytomegalovirus antagonist of type I IFN-dependent signal transducer and activator of transcription signaling. *Proc. Natl. Acad. Sci. U.S.A.* **103**, 3840–3845 (2006).
31. Y. H. Huh *et al.*, Binding STAT2 by thE acidic domain of human cytomegalovirus IE1 promotes viral growth and is negatively regulated by SUMO. *J. Virol.* **82**, 10444–10454 (2008).
32. Y. J. Kim *et al.*, Consecutive inhibition of ISG15 expression and ISGylation by cytomegalovirus regulators. *PLoS Pathog.* **12**, e1005850 (2016).
33. E. Zalckvar *et al.*, Nucleosome maps of the human cytomegalovirus genome reveal a temporal switch in chromatin organization linked to a major IE protein. *Proc. Natl. Acad. Sci. U.S.A.* **110**, 13126–13131 (2013).
34. J. N. Kline, L. J. Geist, M. M. Monick, M. F. Stinski, G. W. Hunninghake, Regulation of expression of the IL-1 receptor antagonist (IL-1ra) gene by products of the human cytomegalovirus immediate early genes. *J. Immunol.* **152**, 2351–2357 (1994).
35. L. J. Geist, M. M. Monick, M. F. Stinski, G. W. Hunninghake, The immediate early genes of human cytomegalovirus upregulate tumor necrosis factor-alpha gene expression. *J. Clin. Invest.* **93**, 474–478 (1994).
36. L. J. Geist, M. M. Monick, M. F. Stinski, G. W. Hunninghake, The immediate early genes of human cytomegalovirus upregulate expression of the interleukin-2 and interleukin-2 receptor genes. *Am. J. Respir. Cell Mol. Biol.* **5**, 292–296 (1991).
37. T. W. Hermiston, C. L. Malone, P. R. Witte, M. F. Stinski, Identification and characterization of the human cytomegalovirus immediate-early region 2 gene that stimulates gene expression from an inducible promoter. *J. Virol.* **61**, 3214–3221 (1987).
38. M. M. Monick, L. J. Geist, M. F. Stinski, G. W. Hunninghake, The immediate early genes of human cytomegalovirus upregulate expression of the cellular genes myc and fos. *Am. J. Respir. Cell Mol. Biol.* **7**, 251–256 (1992).
39. L. J. Geist, M. M. Monick, M. F. Stinski, G. W. Hunninghake, Cytomegalovirus immediate early genes prevent the inhibitory effect of cyclosporin A on interleukin 2 gene transcription. *J. Clin. Invest.* **90**, 2136–2140 (1992).
40. G. K. Iwamoto *et al.*, Modulation of interleukin 1 beta gene expression by the immediate early genes of human cytomegalovirus. *J. Clin. Invest.* **85**, 1853–1857 (1990).
41. R. Caswell, L. Bryant, J. Sinclair, Human cytomegalovirus immediate-early 2 (IE2) protein can transactivate the human hsp70 promoter by alleviation of Dr1-mediated repression. *J. Virol.* **70**, 4028–4037 (1996).
42. D. T. Petrik, K. P. Schmitt, M. F. Stinski, The autoregulatory and transactivating functions of the human cytomegalovirus IE86 protein use independent mechanisms for promoter binding. *J. Virol.* **81**, 5807–5818 (2007).
43. D. M. Lukac, N. Y. Harel, N. Tanese, J. C. Alwine, TAF-like functions of human cytomegalovirus immediate-early proteins. *J. Virol.* **71**, 7227–7239 (1997).
44. R. Caswell *et al.*, The human cytomegalovirus 86K immediate early (IE) 2 protein requires the basic region of the TATA-box binding protein (TBP) for binding, and interacts with TBP and transcription factor TFIIB via regions of IE2 required for transcriptional regulation. *J. Gen. Virol.* **74**, 2691–2698 (1993).
45. A. D. Yurochko, S. M. Huong, E. S. Huang, Identification of human cytomegalovirus target sequences in the human immunodeficiency virus long terminal repeat. Potential role of IE2-86 binding to sequences between -120 and -20 in promoter transactivation. *J. Hum. Virol.* **2**, 81–90 (1999).
46. J. L. Meier, J. A. Pruessner, The human cytomegalovirus major immediate-early distal enhancer region is required for efficient viral replication and immediate-early gene expression. *J. Virol.* **74**, 1602–1613 (2000).
47. L. Hennighausen, B. Fleckenstein, Nuclear factor 1 interacts with five DNA elements in the promoter region of the human cytomegalovirus major immediate early gene. *EMBO J.* **5**, 1367–1371 (1986).
48. M. P. Macias, L. Huang, P. E. Lashmit, M. F. Stinski, Cellular or viral protein binding to a cytomegalovirus promoter transcription initiation site: Effects on transcription. *J. Virol.* **70**, 3628–3635 (1996).
49. G. W. Hunninghake, M. M. Monick, B. Liu, M. F. Stinski, The promoter-regulatory region of the major immediate-early gene of human cytomegalovirus responds to T-lymphocyte stimulation and contains functional cyclic AMP-response elements. *J. Virol.* **63**, 3026–3033 (1989).
50. H. Isomura, M. F. Stinski, The human cytomegalovirus major immediate-early enhancer determines the efficiency of immediate-early gene transcription and viral replication in permissive cells at low multiplicity of infection. *J. Virol.* **77**, 3602–3614 (2003).
51. P. E. Lashmit, C. A. Lundquist, J. L. Meier, M. F. Stinski, Cellular repressor inhibits human cytomegalovirus transcription from the UL127 promoter. *J. Virol.* **78**, 5113–5123 (2004).
52. P. Lashmit, S. Wang, H. Li, H. Isomura, M. F. Stinski, The CREB site in the proximal enhancer is critical for cooperative interaction with the other transcription factor binding sites to enhance transcription of the major intermediate-early genes in human cytomegalovirus-infected cells. *J. Virol.* **83**, 8893–8904 (2009).
53. H. Isomura, T. Tsurumi, M. F. Stinski, Role of the proximal enhancer of the major immediate-early promoter in human cytomegalovirus replication. *J. Virol.* **78**, 12788–12799 (2004).
54. W. A. Bresnahan, T. E. Shenk, UL82 virion protein activates expression of immediate early viral genes in human cytomegalovirus-infected cells. *Proc. Natl. Acad. Sci. U.S.A.* **97**, 14506–14511 (2000).
55. S. R. Cantrell, W. A. Bresnahan, Interaction between the human cytomegalovirus UL82 gene product (pp71) and hDaxx regulates immediate-early gene expression and viral replication. *J. Virol.* **79**, 7792–7802 (2005).
56. I. Cristea *et al.*, Human cytomegalovirus pUL83 stimulates activity of the viral immediate-early promoter through its interaction with the cellular IFI16 protein. *J. Virol.* **84**, 7803–7814 (2010).
57. M. J. Romanowski, E. Garrido-Guerrero, T. Shenk, pIRS1 and pTRS1 are present in human cytomegalovirus virions. *J. Virol.* **71**, 5703–5705 (1997).
58. R. R. Penkert, R. F. Kalejta, Tale of a tegument transactivator: The past, present and future of human CMV pp71. *Future Virol.* **7**, 855–869 (2012).

59. R. M. Stenberg, A. S. Depto, J. Fortney, J. A. Nelson, Regulated expression of early and late RNAs and proteins from the human cytomegalovirus immediate-early gene region. *J. Virol.* **63**, 2699–2708 (1989).
60. D. Collins-McMillen *et al.*, Alternative promoters drive human cytomegalovirus reactivation from latency. *Proc. Natl. Acad. Sci. U.S.A.* **116**, 17492–17497 (2019).
61. K. C. Arend, B. Ziehr, H. A. Vincent, N. J. Moorman, Multiple transcripts encode full-length human cytomegalovirus IE1 and IE2 proteins during lytic infection. *J. Virol.* **90**, 8855–8865 (2016).
62. R. M. Stenberg, P. R. Witte, M. F. Stinski, Multiple spliced and unspliced transcripts from human cytomegalovirus immediate-early region 2 and evidence for a common initiation site within immediate-early region 1. *J. Virol.* **56**, 665–675 (1985).
63. S. Awasthi, J. A. Isler, J. C. Alwine, Analysis of splice variants of the immediate-early 1 region of human cytomegalovirus. *J. Virol.* **78**, 8191–8200 (2004).
64. G. Du, N. Dutta, P. Lashmit, M. F. Stinski, Alternative splicing of the human cytomegalovirus major immediate-early genes affects infectious-virus replication and control of cellular cyclin-dependent kinase. *J. Virol.* **85**, 804–817 (2011).
65. W. Hou *et al.*, Two polypyrimidine tracts in intron 4 of the major immediate early gene are critical for gene expression switching from IE1 to IE2 and for replication of human cytomegalovirus. *J. Virol.* **90**, 7339–7349 (2016).
66. F. P. Martínez *et al.*, CTCF binding to the first intron of the major immediate early (MIE) gene of human cytomegalovirus (HCMV) negatively regulates MIE gene expression and HCMV replication. *J. Virol.* **88**, 7389–7401 (2014).
67. K. C. Arend, E. M. Lenarcic, N. J. Moorman, The 5′ untranslated region of the major immediate early mRNA is necessary for efficient human cytomegalovirus replication. *J. Virol.* **92**, e02128-17 (2018).
68. D. Wang, W. Bresnahan, T. Shenk, Human cytomegalovirus encodes a highly specific RANTES decoy receptor. *Proc. Natl. Acad. Sci. U.S.A.* **101**, 16642–16647 (2004).
69. M. Umashankar *et al.*, A novel human cytomegalovirus locus modulates cell type-specific outcomes of infection. *PLoS Pathog.* **7**, e1002444 (2011).
70. E. A. Pitt *et al.*, The D-form of a novel heparan binding peptide decreases cytomegalovirus infection in vivo and in vitro. *Antiviral Res.* **135**, 15–23 (2016).
71. H. A. Vincent, B. Ziehr, N. J. Moorman, Mechanism of protein kinase R inhibition by human cytomegalovirus pTRS1. *J. Virol.* **91**, e01574-16 (2017).
72. H. Zhu, Y. Shen, T. Shenk, Human cytomegalovirus IE1 and IE2 proteins block apoptosis. *J. Virol.* **69**, 7960–7970 (1995).
73. M. Umashankar *et al.*, Antagonistic determinants controlling replicative and latent states of human cytomegalovirus infection. *J. Virol.* **88**, 5987–6002 (2014).
74. M. C. Silva, Q.-C. Yu, L. Enquist, T. Shenk, Human cytomegalovirus UL99-encoded pp28 is required for the cytoplasmic envelopment of tegument-associated capsids. *J. Virol.* **77**, 10594–10605 (2003).
75. M. J. Romanowski, T. Shenk, Characterization of the human cytomegalovirus irs1 and trs1 genes: A second immediate-early transcription unit within irs1 whose product antagonizes transcriptional activation. *J. Virol.* **71**, 1485–1496 (1997).
76. S. Terhune *et al.*, Human cytomegalovirus UL38 protein blocks apoptosis. *J. Virol.* **81**, 3109–3123 (2007).
77. E. M. Lenarcic, B. Ziehr, G. De Leon, D. Mitchell, N. J. Moorman, Differential role for host translation factors in host and viral protein synthesis during human cytomegalovirus infection. *J. Virol.* **88**, 1473–1483 (2014).
78. L. Rank, L. E. Herring, M. Braunstein, Evidence for the mycobacterial Mce4 Transporter being a multiprotein complex. *J. Bacteriol.* **203**, e00685-20 (2021).
79. S. Tyanova *et al.*, The Perseus computational platform for comprehensive analysis of (prote)omics data. *Nat. Methods* **13**, 731–740 (2016).
80. E. M. Lenarcic, B. J. Ziehr, N. J. Moorman, An unbiased proteomics approach to identify human cytomegalovirus RNA-associated proteins. *Virology* **481**, 13–23 (2015).
81. O. O. Abudayyeh *et al.*, RNA targeting with CRISPR-Cas13. *Nature* **550**, 280–284 (2017).
82. D. B. T. Cox *et al.*, RNA editing with CRISPR-Cas13. *Science* **358**, 1019–1027 (2017).
83. L.-Z. Yang *et al.*, Dynamic imaging of RNA in living cells by CRISPR-Cas13 systems. *Mol. Cell* **76**, 981–997.e7 (2019).
84. W. Qin, K. F. Cho, P. E. Cavanagh, A. Y. Ting, Deciphering molecular interactions by proximity labeling. *Nat. Methods* **18**, 133–143 (2021).
85. B. Dickmander *et al.*, Specific RNA structures in the 5′ untranslated region of the human cytomegalovirus major immediate early transcript are critical for efficient virus replication. *mBio* **15**, e0262123 (2024).
86. E. M. Lenarcic, N. J. Moorman, Data from "Novel RNA-targeted proteomics approach leads to the identification of a key role for YBX1 in HCMV replication." ProteomeXchange. https://www.ebi.ac.uk/pride/archive/projects/PXD054962. Deposited 16 August 2024.
87. M. Winkler, S. A. Rice, T. Stamminger, UL69 of human cytomegalovirus, an open reading frame with homology to ICP27 of herpes simplex virus, encodes a transactivator of gene expression. *J. Virol.* **68**, 3943–3954 (1994).
88. P. Lischka, Z. Toth, M. Thomas, R. Mueller, T. Stamminger, The UL69 transactivator protein of human cytomegalovirus interacts with DEXD/H-Box RNA helicase UAP56 to promote cytoplasmic accumulation of unspliced RNA. *Mol. Cell. Biol.* **26**, 1631–1643 (2006).
89. Z. Toth, P. Lischka, T. Stamminger, RNA-binding of the human cytomegalovirus transactivator protein UL69, mediated by arginine-rich motifs, is not required for nuclear export of unspliced RNA. *Nucleic Acids Res.* **34**, 1237–1249 (2006).
90. K. S. Colletti, K. E. Smallenburg, Y. Xu, G. S. Pari, Human cytomegalovirus UL84 interacts with an RNA stem–loop sequence found within the RNA/DNA hybrid region of oriLyt. *J. Virol.* **81**, 7077–7085 (2007).
91. J. Dong *et al.*, RNA-binding specificity of Y-box protein 1. *RNA Biol.* **6**, 59–64 (2009).
92. H. Goodarzi *et al.*, Endogenous tRNA-derived fragments suppress breast cancer progression via YBX1 displacement. *Cell* **161**, 790–802 (2015).
93. E. Kwon *et al.*, The RNA-binding protein YBX1 regulates epidermal progenitors at a posttranscriptional level. *Nat. Commun.* **9**, 1734 (2018).
94. J. A. Lindquist, P. R. Mertens, Cold shock proteins: From cellular mechanisms to pathophysiology and disease. *Cell Commun. Signal.* **16**, 63 (2018).
95. X. Liu *et al.*, RNA m5C modification upregulates E2F1 expression in a manner dependent on YBX1 phase separation and promotes tumor progression in ovarian cancer. *Exp. Mol. Med.* **56**, 600–615 (2024).
96. D. N. Lyabin, I. A. Eliseeva, L. P. Ovchinnikov, YB-1 protein: Functions and regulation. *WIREs RNA* **5**, 95–110 (2014).
97. D. Mordovkina *et al.*, Y-box binding proteins in mRNP assembly, translation, and stability control. *Biomolecules* **10**, 591 (2020).
98. A. M. El-Naggar *et al.*, Class I HDAC inhibitors enhance YB-1 acetylation and oxidative stress to block sarcoma metastasis. *EMBO Rep.* **20**, e48375 (2019).
99. S. P. Somasekharan *et al.*, YB-1 regulates stress granule formation and tumor progression by translationally activating G3BP1. *J. Cell Biol.* **208**, 913–929 (2015).
100. Y. Ban *et al.*, RNA-binding protein YBX1 promotes cell proliferation and invasiveness of nasopharyngeal carcinoma cells via binding to AURKA mRNA. *J. Cancer* **12**, 3315–3324 (2021).
101. R. Wu *et al.*, Transcriptional and post-transcriptional control of autophagy and adipogenesis by YBX1. *Cell Death Dis.* **14**, 1–13 (2023).
102. Z.-L. Li *et al.*, HCV 5-methylcytosine enhances viral RNA replication through interaction with m5C reader YBX1. *ACS Chem. Biol.* **19**, 1648–1660 (2024), 10.1021/acschembio.4c00322.
103. S. M. Paranjape, E. Harris, Y box-binding protein-1 binds to the dengue virus 3′-untranslated region and mediates antiviral effects. *J. Biol. Chem.* **282**, 30497–30508 (2007).
104. L. Chatel-Chaix *et al.*, A host YB-1 ribonucleoprotein complex is hijacked by hepatitis C virus for the control of NS3-dependent particle production. *J. Virol.* **87**, 11704–11720 (2013).
105. X. Mu, W. Li, X. Wang, G. Gao, YB-1 stabilizes HIV-1 genomic RNA and enhances viral production. *Protein Cell* **4**, 591–597 (2013).
106. D. V. Bann, A. R. Beyer, L. J. Parent, A murine retrovirus co-Opts YB-1, a translational regulator and stress granule-associated protein, to facilitate virus assembly. *J. Virol.* **88**, 4434–4450 (2014).
107. M. Hakki, A. P. Geballe, Double-stranded RNA binding by human cytomegalovirus pTRS1. *J. Virol.* **79**, 7311–7318 (2005).
108. C. J. Bierle, K. M. Semmens, A. P. Geballe, Double-stranded RNA binding by the human cytomegalovirus PKR antagonist TRS1. *Virology* **442**, 28–37 (2013).
109. B. Ziehr *et al.*, Human cytomegalovirus TRS1 protein associates with the 7-methylguanosine mRNA cap and facilitates translation. *Proteomics* **15**, 1983–1994 (2015).
110. H. A. Vincent, B. Ziehr, E. Lenarcic, N. J. Moorman, Human cytomegalovirus pTRS1 stimulates cap-independent translation. *Virology* **537**, 246–253 (2019).
111. M. Aoyagi, M. Gaspar, T. E. Shenk, Human cytomegalovirus UL69 protein facilitates translation by associating with the mRNA cap-binding complex and excluding 4EBP1. *Proc. Natl. Acad. Sci. U.S.A.* **107**, 2640–2645 (2010).
112. B. Ziehr, E. Lenarcic, C. Cecil, N. J. Moorman, The eIF4AIII RNA helicase is a critical determinant of human cytomegalovirus replication. *Virology* **489**, 194–201 (2016).
113. H. Meng *et al.*, YBX1 promotes homologous recombination and resistance to platinum-induced stress in ovarian cancer by recognizing m5C modification. *Cancer Lett.* **597**, 217064 (2024).
114. V. Evdokimova *et al.*, Translational activation of snail1 and other developmentally regulated transcription factors by YB-1 promotes an epithelial–mesenchymal transition. *Cancer Cell* **15**, 402–415 (2009).
115. A. M. El-Naggar *et al.*, Translational activation of HIF1α by YB-1 promotes sarcoma metastasis. *Cancer Cell* **27**, 682–697 (2015).
116. L. C. Cobbold *et al.*, Upregulated c-myc expression in multiple myeloma by internal ribosome entry results from increased interactions with and expression of PTB-1 and YB-1. *Oncogene* **29**, 2884–2895 (2010).
117. L. C. Cobbold *et al.*, Identification of internal ribosome entry segment (IRES)-trans-acting factors for the Myc family of IRESs. *Mol. Cell. Biol.* **28**, 40–49 (2008).
118. T. Tanaka, S. Ohashi, S. Kobayashi, Roles of YB-1 under arsenite-induced stress: Translational activation of HSP70 mRNA and control of the number of stress granules. *Biochim. Biophys. Acta* **1840**, 985–992 (2014).
119. J. A. Isler, A. H. Skalet, J. C. Alwine, Human cytomegalovirus infection activates and regulates the unfolded protein response. *J. Virol.* **79**, 6890–6899 (2005).